SGP-TR-32

STANFORD GEOTHERMAL PROGRAM

PROGRESS REPORT NO. 7

to

U. S. DEPARTMENT OF ENERGY

LAWRENCE BERKELEY LABORATORY

for the period

October 1, 1978 through December 31, 1978

Contract DOE-LBL-167-3500

Paul Kruger and Henry J. Ramey, Jr.
Co-Principal Investigators
Stanford University
Stanford, CA 94305

TABLE OF CONTENTS

INTRODUCTION

This Seventh Quarterly Progress Report covers the contract period from October 1, 1978 through December 31, 1978. Research is performed under the Department of Energy Contract DOE-LBL-167-3500 with Lawrence Berkeley Laboratory, effective June 1, 1977.

Although not entirely complete, the suite of SGP papers prepared for the Fourth Workshop represents an excellent cross section of the many projects completed or underway since the Third Workshop in December, 1977. Accordingly, this quarterly report consists of the collection of Summary presentations prepared by the Stanford Geothermal Program staff. Included with these Summaries is the paper by Barelli, et al, which describes some of the efforts under the ENEL-DOE project at Stanford. To complete the review of the major projects in the Stanford Geothermal Program, the two-part Abstract on the presentation of the fractured-rock physical model energy-recovery project, submitted to the ASME-AIChE National Heat Transfer Conference, is included in this quarterly report. Finally, a number of papers were prepared for the Fall meeting, Society of Petroleum Engineers of AIME. Copies of these papers, listed in the Well Test Analysis Section of this report, are available.

In view of the more-detailed descriptions of the scope of the projects covered in these Summaries, this quarterly report is being prepared as a SGP technical report and will be given wider circulation than previous quarterly reports.

PROJECT **SUMMARIES**

RECENT BENCH-SCALE EXPERIMENTS

J.R. Counsil, C.H. Hsieh, C. Ehlig-Economides, A. Danesh and H.J. Ramey, Jr.

The Stanford Geothermal Project bench-scale experiments are designed to improve the understanding of geothermal reservoir physics. Three sets of experiments are discussed in the following sections: (1) vapor pressure lowering in porous media due to capillarity and adsorption, (2) the effect of temperature on absolute permeability, and (3) the determination of steam-water relative permeability for drainage processes.

Vapor Pressure Lowering

Vapor pressure lowering in porous media may be important to both reserve evaluation and geothermal reservoir performance prediction. Vapor pressure lowering is a lowering of the vapor pressure curve. As shown schematically in Fig. 1, it occurs at low water saturations. The lowering may be caused by (1) capillarity, i.e., curved liquid-vapor interfaces in porous media and/or by (2) surface adsorption of fluid molecules at the solid-fluid interface. It is believed that capillary effects occur at low water saturations, but that vapor pressure lowering is minor until saturations are so low that adsorption phenomena dominate (Hsieh et al., 1978).

The importance of vapor pressure lowering is further demonstrated by the following hypothetical situation. If the temperature and pressure of a geothermal reservoir are determined to be that of point A in Fig. 1, a reservoir engineer may use the flat surface vapor pressure curve and assume the reservoir is 100% dry steam and contains no liquid water. In actual practice, further lowering of reservoir pressure may allow capillary or adsorbed water to vaporize. Thus, both the reserves and the rate of production are increased beyond that predicted with the assumption of no vapor pressure lowering (and no liquid water saturation).

The following calculation demonstrates the possible importance of surface adsorption. A reservoir rock of 1 m^2/gm surface area, 25% porosity, and 10.6 $Å^2$ surface area per H_2O molecule will have 7.95 m^2 surface area per cc pore volume and 2.24×10^{-3} gm H_2O per cc pore volume.

At the arbitrary condition of 200°C and 15 bars, saturated steam density (should use superheated) is .00786 gm H_2O/cc. Using the above unconfirmed assumptions, one layer of adsorbed H_2O will increase reservoir water content by 29%. Ten layers of adsorbed H_2O will further increase

reservoir water content. One unanswered question remains: "How much of the adsorbed H_2O can be produced?

The experimental apparatus required for this study is now assembled. Vapor pressure lowering will be determined as a function of pressure, temperature, and amount of H_2O, using the apparatus shown in Fig. 2. However, it is expected that at each temperature level studied, results will demonstrate multilayer adsorption "plateaus" as shown in Fig. 3. To better understand the adsorption phenomena and to try to estimate the number of adsorption layers, the BET cell shown in Fig. 4 has already been used to determine nitrogen surface areas of consolidated sandstones (Berea) and unconsolidated sand packs. These studies may be extended to include natural gas adsorption phenomena as they occur in natural gas reservoirs.

Effect of Temperature on Absolute Permeability

Experimental results of Weinbrandt (1972), Cassé (1974), Aruna (1976), and others suggest the absolute permeability of sandstones and unconsolidated sands to water is reduced up to 65% at elevated temperatures and confining pressures. Permeability reductions with increased temperature were not observed for nitrogen, oil, or octonol. In addition, permeability reduction was not observed for water flowing through limestone. Recently, Dr. A. Danesh, visiting professor from Abadan Institute of Technology, Iran, performed additional experiments flowing water and oil through unconsolidated sand and unconsolidated stainless steel. His results were similar to those of Cassé and Aruna, but similar reductions in permeability also occurred €or unconsolidated stainless steel (Danesh et al., 1978).

Subsequent experiments were recently completed using water and either unconsolidated sand or limestone ground and sieved to a similar mesh size. These experiments did not reproduce the temperature level effects. The reason the results were different may be due to a different experimental procedure. In particular, water was pumped through the core during the entire experiment. In the earlier experiments, water may not have flowed through the core during heating and cooling between measurements at different temperatures. The solid-liquid boundary layer, intermolecular force mechanism, as suggested by Danesh to explain the permeability reductions, may indicate that such procedural differences are important. Future experiments will attempt to verify Danesh's conclusions.

Steam-Water Relative Permeability

Steam and liquid relative permeabilities, expressed as a function of liquid saturation, are required in the numerical models used to calculate mass and energy recovery from two-phase geothermal reservoirs. Currently, modified Corey-type equations are used because adequate techniques for determining proper steam-water relative permeabilities are still under development. Relative permeabilities are often expressed as equations for convenience.

Sufficient data can be obtained from steady, two-phase, non-isothermal flow experiments to allow the construction of steam-water relative permeability curves for a drainage process. Water saturation can be measured with a capacitance probe (Chen et al., 1978). A preliminary relative permeability curve is shown in Fig. 5. The data has not been corrected for temperature or Klinkenberg slip effects, and the core has not yet been analyzed for nonhomogeneity caused by possible hydrothermal alteration.

In addition, isothermal nitrogen-displacing-water experiments were performed to provide gas-water drainage relative permeabilities at a variety of temperatures. These gas-water relative permeabilities provide an interesting comparison to the steam-water relative permeabilities. One example is shown in Fig. 6. Data analysis is not yet complete, and differences between the two curves have not yet been explained. Stewart et al. (1953) has stated that gas-expansion and gas drive drainage relative permeabilities are identical for hydrocarbons in homogeneous sandstone cores. For this reason, the steam-water and the nitrogen-water experiments are expected to yield similar, and possibly identical, results. Future effort will focus on refining the quality of data obtained from these two types of experiments.

References

Aruna, M.: "The Effects of Temperature and Pressure on Absolute Permeability of Limestone," Ph.D. Dissertation, Stanford University, 1976.

Cassé, F.J.: "The Effect of Temperature and Confining Pressure on Fluid Flow Properties of Consolidated Rocks," Ph.D. Dissertation, Stanford University, 1974.

Chen, H.K., Counsil, J.R., and Ramey, H.J., Jr.: "Experimental Steam-Water Relative Permeability Curves," Geothermal Resources Council Transactions (1978), 2, 103-104.

Danesh, A., Ehlig-Economides, C., and Ramey, H.J., Jr.: "The Effect of Temperature Level on Absolute Permeability of Unconsolidated Silica and Stainless Steel," Geothermal Resources Council Transactions (1978), 2, 137-139.

Hsieh, C.H., and Ramey, H.J., Jr.: "An Inspection of Experimental Data on Vapor Pressure Lowering in Porous Media," Geothermal Resources Council Transactions (1978), 2, 295-296.

Stewart, C.R., Craig, F.F., Jr., and Morse, R.A.: "Determination of Limestone Performance Characteristics by Model Flow Tests," Trans. AIME (1953), 198, 93-102.

Weinbrandt, R.M., Cassé, F.J., and Ramey, H.J., Jr.: "The Effect of Temperature on Relative and Absolute Permeability of Sandstones," Soc. Pet. Eng. J. (Oct. 1975), 376.

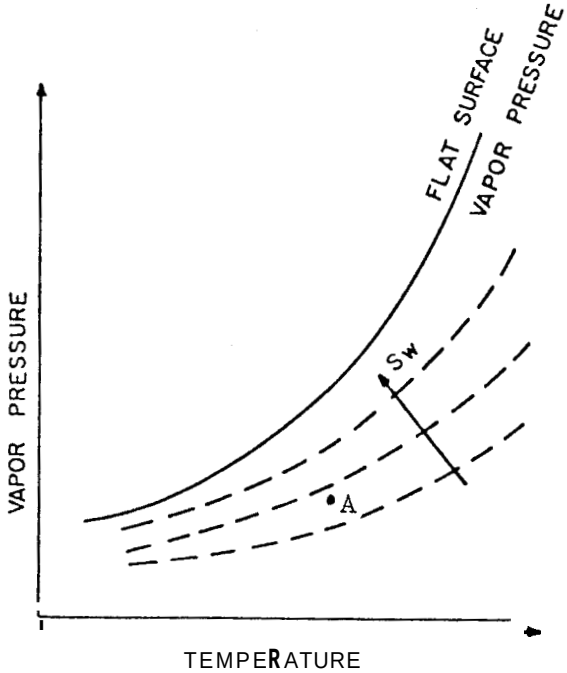

FIGURE 1. HYPOTHETICAL VAPOR PRESSURE CURVE DEPENDENCE ON WATER SATURATION (S_W)

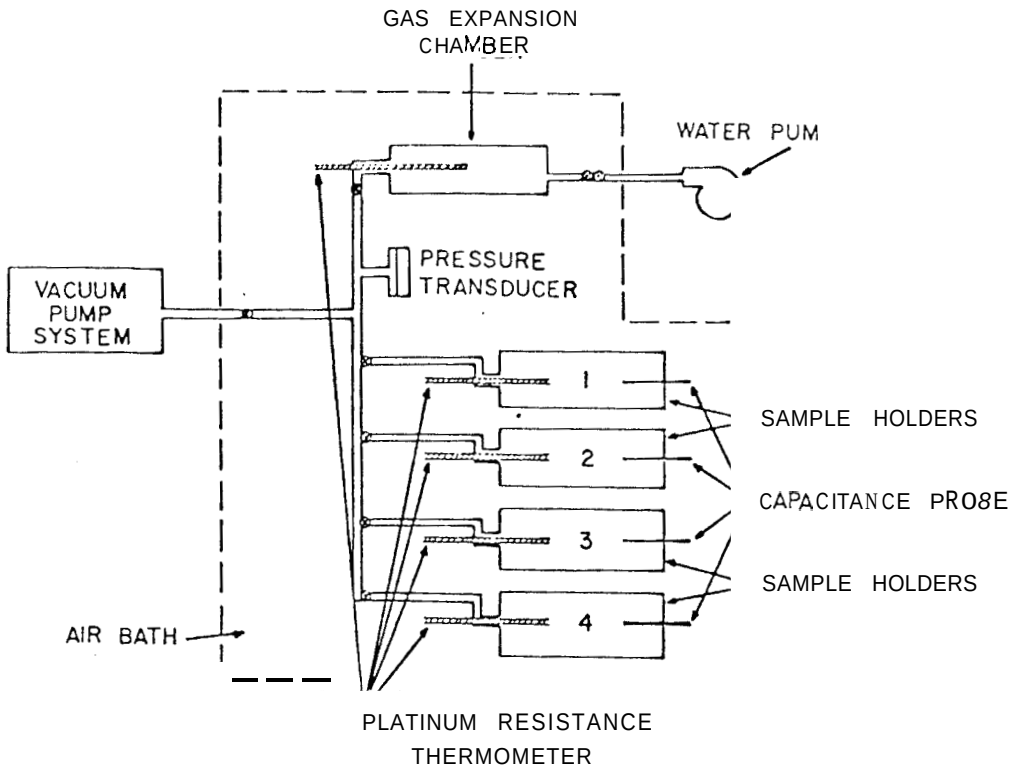

FIGURE 2. APPARATUS USED TO DETERMINE WATER ADSORPTION AND VAPOR PRESSURE LOWERING

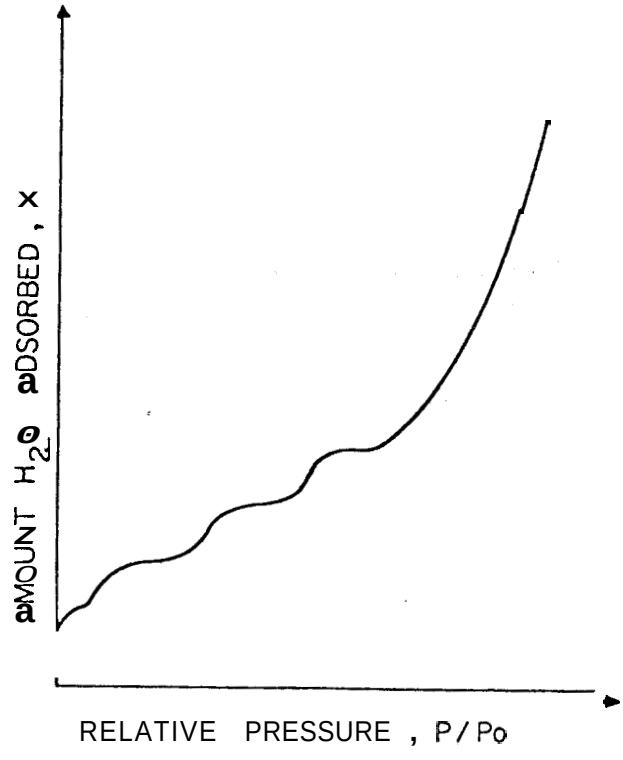

FIGURE 3, SCHEMATIC FIGURE SHOWING AN ADSORPTION ISOTHERM FOR H_2O - S_iO_2

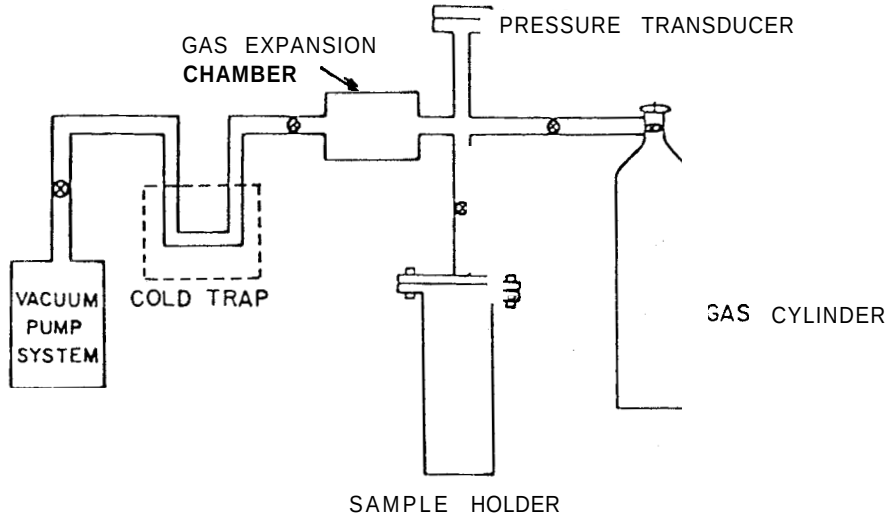

FIGURE 4. BET CELL USED TO DETERMINE ROCK SURFACE AREA

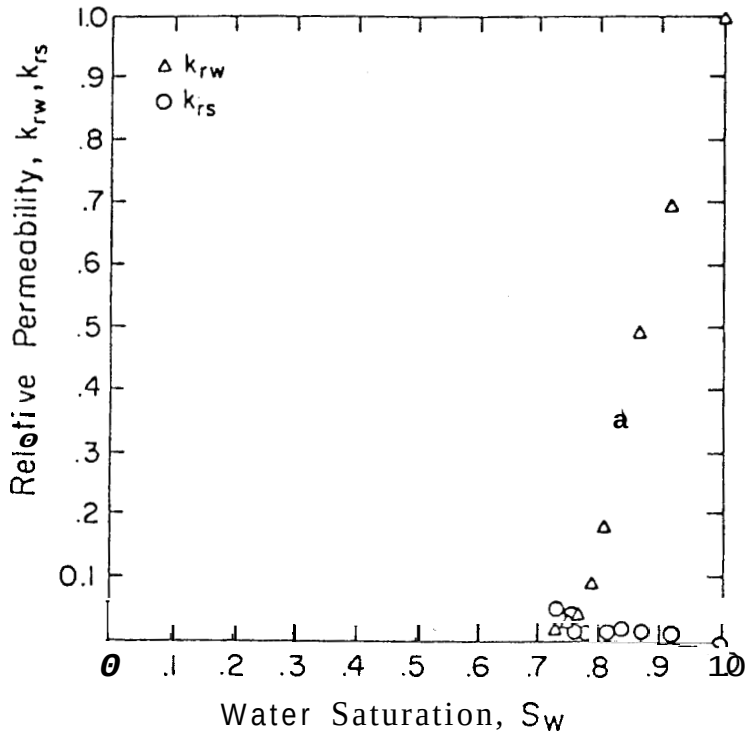

FIGURE 5. STEAM-WATER RELATIVE PERMEABILITY DETERMINED FROM NONISOTHERMAL, BOILING FLOW EXPERIMENT (330-280°F)

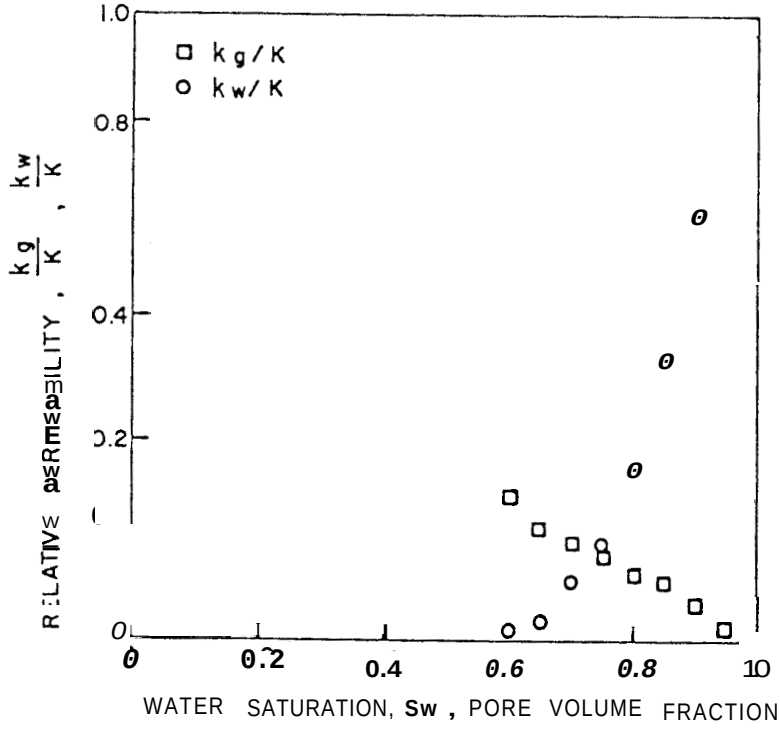

FIGURE 6. NITROGEN-WATER RELATIVE PERXEABILITY DETERMINED FROM ISOTHERMAL GAS-DRIVE EXPERIMENT (300°F)

PRESSURE DRAWDOWN ANALYSIS FOR THE TRAVALE 22 WELL

A. Barelli, W.E. Brigham, H. Cinco, M. Economides, F.G. Miller
H.J. Ramey, Jr., and A. Schultz

Introduction

This work presents preliminary results on the analysis of drawdown data for Travale 22. Both wellhead pressure and flow rate data were recorded in this well for over a period of almost two years.

In the past, Barelli et al. (1975) and Atkinson et al. (1977) presented the analysis of five pressure buildup tests. Figure 1 shows the Horner plot for these cases. They found that to have a good match in all cases, it was necessary to assume that the Travale 22 well is intersected by a partially penetrating vertical fracture in a parallelepiped whose bottom side is maintained at constant pressure (boiling front), as shown in Fig. 2.

Atkinson et al. also presented an analysis for a pressure interface test run in the Travale-Radicondoli area. In this case, the Travale 22 well was flowing and the pressure recorded at wells R1, R3, R5, R6, R9, and Chl (see Fig. 3). Analysis of these data showed that pressure interference in this reservoir can be matched by considering pure linear flow (Figs. 4 and 5). This indicated the possible presence of a vertical fracture intersecting the Travale 22 well. It was determined that fracture is oriented along the N73°W direction. In addition, the pressure interference data showed that no boundary exists within 2 kilometers from the fracture plane. It was mentioned that linear flow should take place in both horizontal and vertical directions.

Analysis of Drawdown Data

As mentioned previously, both wellhead pressure and flow rate were measured when this well was continuously flowing during almost two years. First the bottomhole pressure was calculated and plotted on a semilog paper (Fig. 6). Data on this graph show a curve of increasing slope similar to a fractured well case. The pressure seems to stabilize at 400 days, indicating a possible constant pressure boundary.

A log-log graph of the pressure data is shown in Pig. 7. It can be seen that the first data points follow a one-half slope straight line, suggesting linear flow.

Since previous buildup analysis and interference analysis suggested that the well is intersected by a fracture and the reservoir has a constant pressure boundary, two models are used to analyze the pressure drawdown data:

1) a well intersected by a fully penetrating vertical fracture in a finite system (Gringarten, Ramey, and Raghavan), and,

2) a well intersected by a partially penetrating vertical fracture in a parallelepiped whose bottom side is a constant pressure boundary.

Figure 8 presents the application of the type-curve matching technique by using the first model. Agreement between most of the pressure data and the dimensionless pressure curve is good; however, at very long time (about 400 days), the system seems to reach steady-state flow, indicating the existence of a constant pressure boundary.

Figure 9 presents the match of data with the second flow model (parallelepiped model). The data appears to match the curve for dimensionless formation thickness ≈ 2.5.

Results from this analysis and from previous work are summarized in Table I. It can be seen that although both the results from buildup and drawdown analysis suggest the same type of geometry for the system, they do not agree regarding the dimensions of the reservoir.

Further effort is needed in the analysis of additional drawdown data not presented in this work. At this point, the results from the buildup data are more reliable because the analysis was based on several tests.

Conclusions

A preliminary analysis of the drawdown data for the Travale 22 well seems to indicate the following:

1) the well is intersected by a highly conductive fracture, as found from the buildup and interference data, and

2) a constant pressure boundary seems to exist, causing the system to reach pseudosteady flow at about 400 days.

References

Atkinson, P., Barelli, A., Brigham, W.E., Celati, R., Manetti, G., Miller, F., Nery, G., and Ramey, H.J., Jr.: "Well-Testing in Travale-Radicondoli Field," Proc., Lardarello Workshop on Geothermal Resource Assessment and Reservoir Engineering, Pisa, Italy, Sept. 12-16, 1977.

Barelli, A., Celati, R., Manetti, G., and Neri, G.: "Horner's Method Applied to Buildup Tests on Travale 22 Well," Summaries of the Second Workshop on Geothermal Reservoir Engineering, Stanford University, Stanford, California, Dec. 15-17, 1975.

Nomenclature

c_t = compressibility (Kg/cm2)-1

h = reservoir thickness (m)

k = permeability (m)

p = pressure (Kg/cm2)

q = flow rate (tons/hour)

t = time (days)

x_f = half fracture length (m)

ϕ = porosity

μ = viscosity (cp)

TABLE I: RESULTS FROM PRESSURE TESTS

	kx_fh_f (Darcy m2)	$\phi h_f x_f$ (m2)
Interference	$5x10^4$	$1.5x10^4$
Buildup	$2.5x10^5k$	$2.5x10^4$ (ϕ=.1)
Drawdown (Parallelepiped)	$1.4x10^3$ (ϕ=.1)	$1.2x10^4$ (ϕ=.1)
Drawdown (Vertical Fracture)	$6.552\ x_f$	$3.66x10^6/x_f$

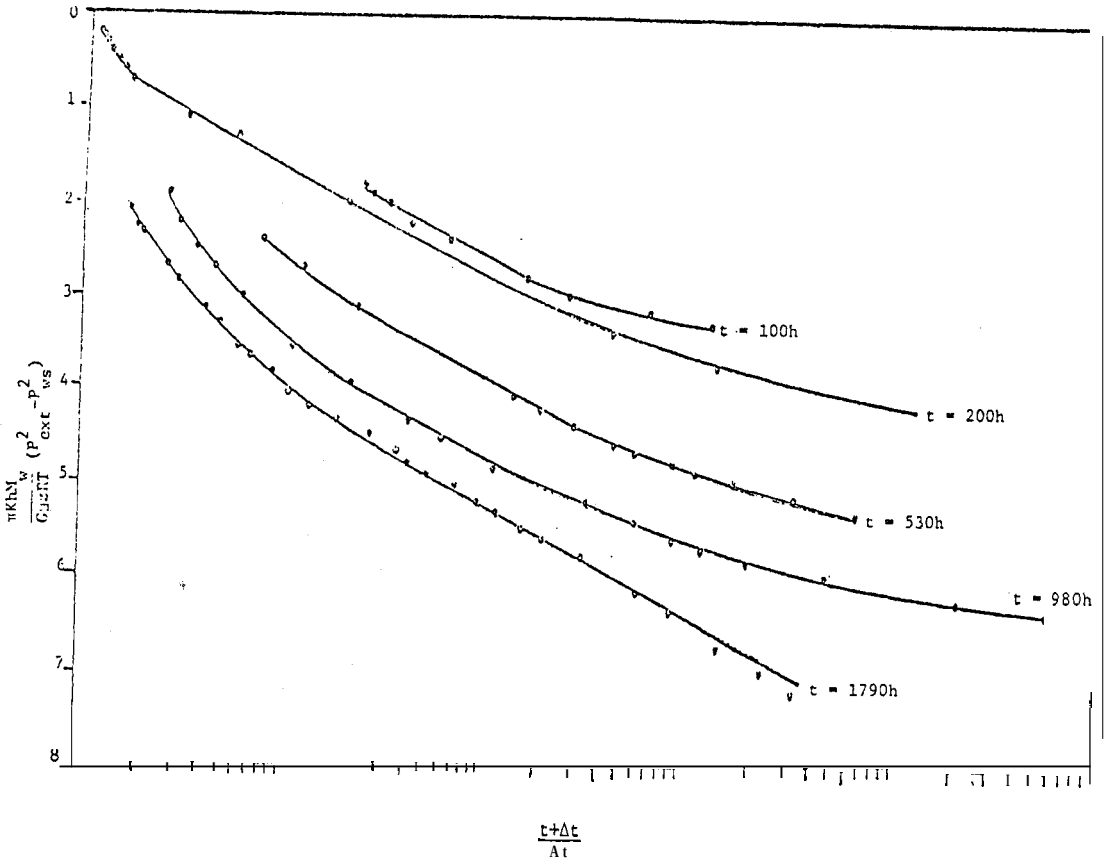

FIG. 1: RECONSTRUCTED HORNER BUILDUP GRAPH FOR T-22 WELL, 1972–1973 (Barelli et al., 1975)

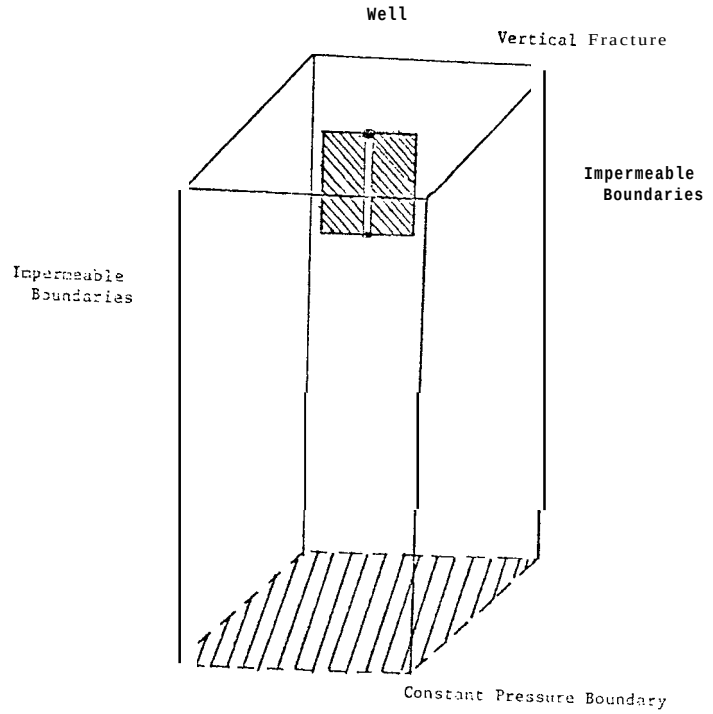

FIG. 2: PARALLELEPIPED MODEL FOR A WELL INTERSECTED BY A PARTIALLY PENETRATING VERTICAL FRACTURE

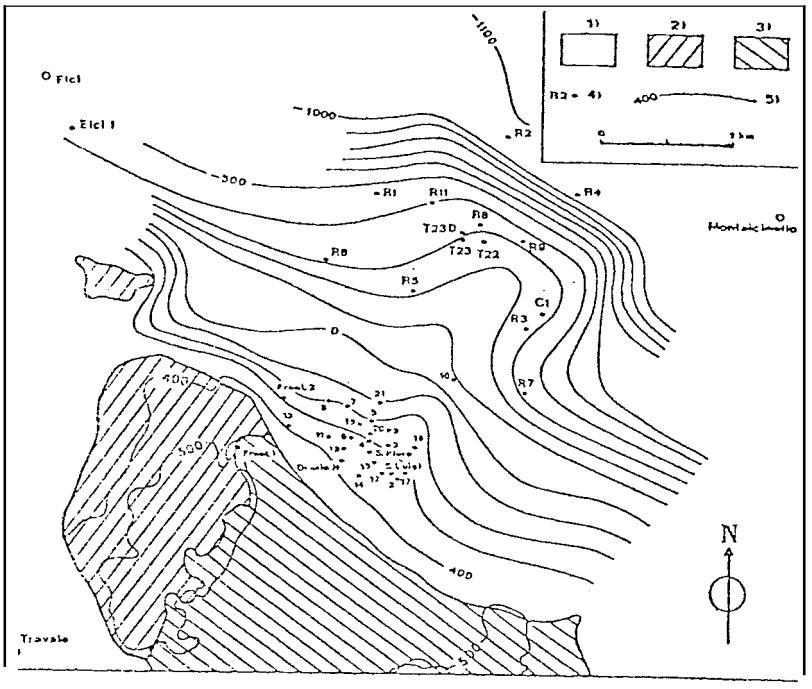

FIG. 3: TRAVALE GEOTHERMAL FIELD. STRUCTURAL MAP OF THE RESERVOIR TOP.
1: COVER COMPLEX: 2: RADIOLARITES AND LIMESTONES (PREDOMINATING);
3: CAVERNOUS LIMESTONES; 4: WELLS; 5: ISOBATHS (ELEVATION m a.s.l.)

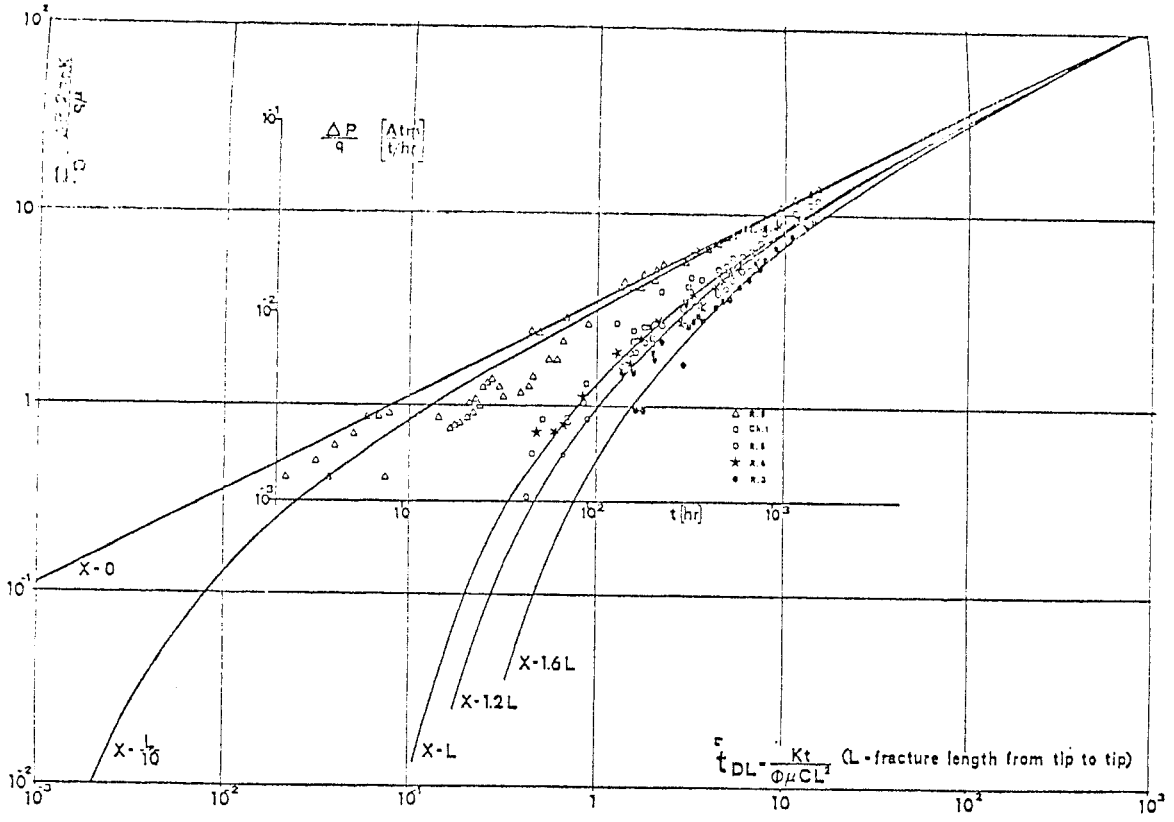

FIG. 4: INTERFERENCE DATA MATCHED WITH TYPE CURVES (Atkinson et al.)

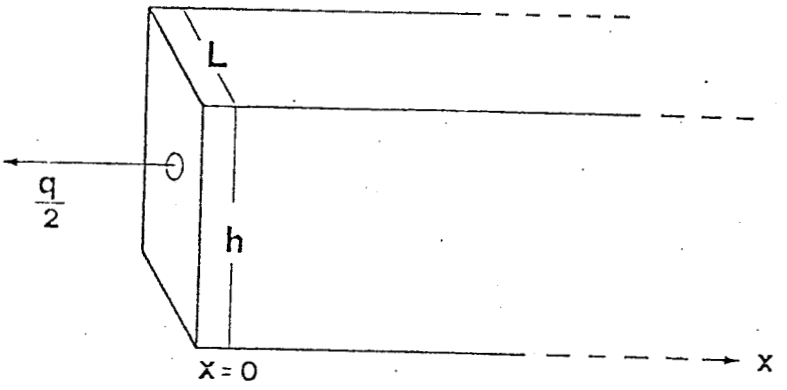

FIG. 5: LINEAR FLOW GEOMETRY (Atkinson et al.)

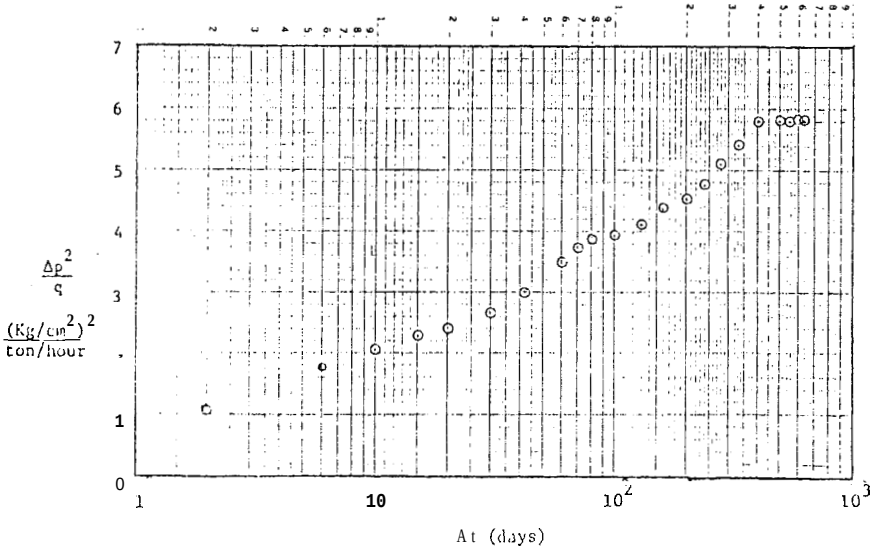

FIG. 6: SEMILOGARITHMIC PLOT FOR THE TRAVALE 22 WELL DRAWDOWN DATA

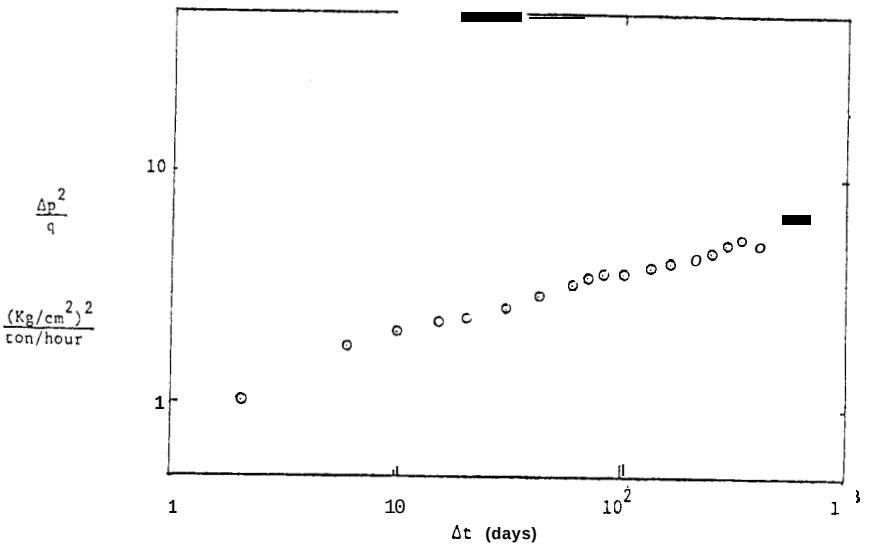

FIG. 7: LOG-LOG GRAPH OF DRAWDOWN DATA

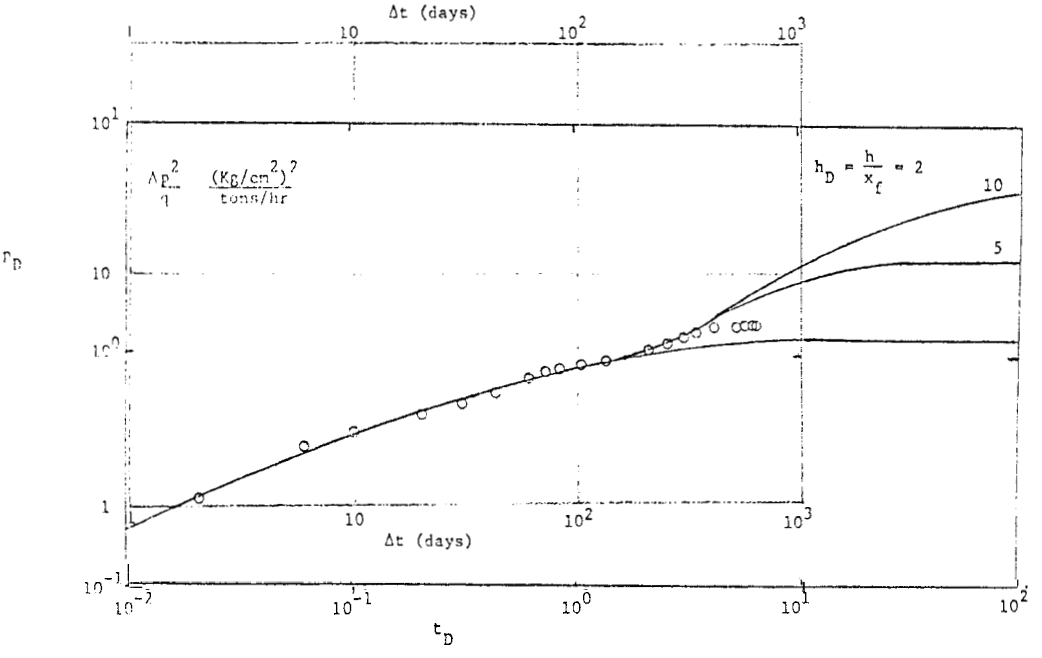

FIG. 8· TYPE-CURVE MATCHING WITH PARALLELEPIPED MODEL

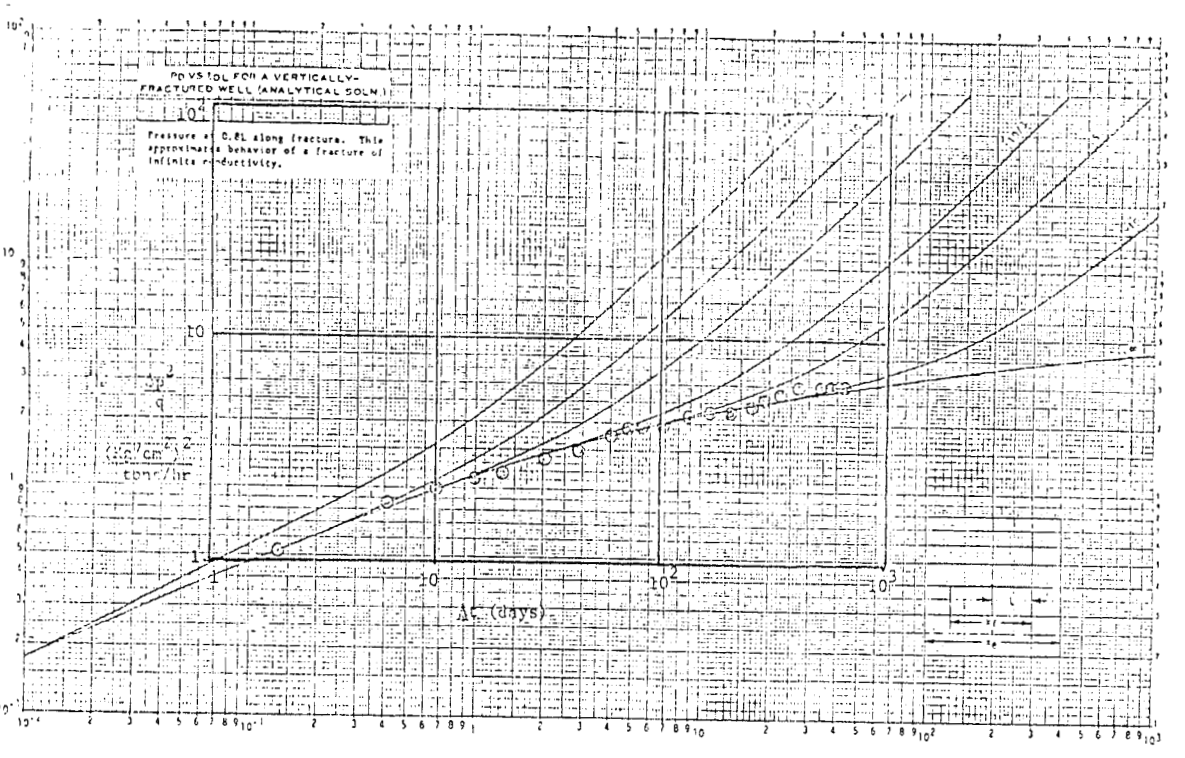

FIG. 9: TYPE-CURVE MATCH FOR THE DRAWDOWN DATA BY USING THE INFINITE CONDUCTIVITY VERTICAL FRACTURE SOLUTION

RECENT DEVELOPMENTS IN WELL TEST ANALYSIS

C. Ehlig-Economides

In the past year a number of studies pertaining to geothermal well test analysis were conducted. In this paper a brief overview of progress on the following six subjects is presented: (1) earth tide effects on a closed reservoir, (2) transient pressure analysis of multilayered heterogeneous reservoirs, (3) interference testing with wellbore storage and skin at the producing well, (4) steam/water relative permeabilities, (5) transient rate and pressure buildup resulting from constant pressure production, and (6) transient pressure analysis of a parallelepiped reservoir.

Earth Tide Effects

The gravitational attraction between the sun, moon, and earth induces a radial deformation of the earth which results in the readily observable oceanic tides. The same mechanism also generates a state of stress on the surface of the earth which has been referred to as earth tides. Due to the low compressibility of the earth compared to that of water, the pressure transients caused by earth tides are of small amplitude. However, the pressure changes are of sufficient magnitude to cause water level variations in open wells and pits, and several investigators have indicated that a relationship exists between the amplitude of the response of an open well system and the characteristics of the formation and the fluid contained therein.

P. Arditty[1,2] modified the equations solved by Bodvarsson[3] for an open well in a finite closed reservoir to apply to a shut-in well with the borehole completely filled with formation fluid. Only one phase is flowing in the reservoir, and the reservoir is confined and infinite in radial extent. The expression for pressure induced by an applied tectonic pressure, p_c, is given by:

$$p = p_{SD}\left(1 - \frac{ae^{n(a-r)}}{r\left[1+\frac{B}{i\omega}\left(\frac{1}{a}+n\right)\right]}\right) \qquad (1)$$

with:

$$p_a = p_{SD}\left(1 - \frac{1}{1+\frac{B}{i\omega a}(na+1)}\right) \qquad (2)$$

where $B = 4k/c_f\mu\ell$, $n^2 = i\omega/d$, ω = oscillation frequency, d = diffusivity $k/\phi\mu c$, a = wellbore radius, and r = radial distance from well. The static-pressure $p_{SD} = p_c(4G_m c_f - c_m)/(3+4G_m c_f)$, where p_c is an applied tectonic pressure, G_m is the rock matrix shear modulus, c_f is fluid compressibility, and c_m is matrix compressibility. The amplitude of the relative response p_a/p_{SD} is:

$$R_e(p_a/p_{SD}) \cong R_e\left(\frac{4k/i\omega\mu a\ell c_f}{1 - \frac{4k}{i\omega\mu a\ell c_f}}\right) \qquad (3)$$

The critical frequency, ω_c, for which the response amplitude exhibits an abrupt decrease is defined by:

$$\omega_c = \frac{4k}{\mu a\ell c_f} \qquad (4)$$

Tides are classified according to length of period, T: long period tides (T = 16 days); diurnal tides (T = 1 day), semidiurnal tides (T = 1/2 day); and terdiurnal tides (T = 1/3 day). If $\omega_c/2\pi >> 2$, then the critical frequency exceeds both the diurnal and semidiurnal frequencies, and $A_D/A_{SD} \simeq 1$, where A_D and A_{SD} are the diurnal and semidiurnal amplitudes of the earth tide effect. If $1 < \omega_c/2\pi < 2$, then $1.25 < A_D/A_{SD} < 2$. If $\omega_c/2\pi << 1$, both amplitudes will be small, and undetectable. Thus, the ratio of the two amplitudes determines limits on the value of ω_c, which in turn gives an approximation for $k/\mu c_f$ since a and ℓ are known. If ω_c is computed from $k/\mu c_f$, an explanation for existence or nonexistence of tidal effects is provided.

A graph of amplitude versus period for a typical sandstone reservoir containing gas is shown in Fig. 1. From these results we would expect the diurnal tide amplitude to exceed the semidiurnal tide amplitude and both should be detectable.

Figure 3 shows raw data from a fluid test. Figure 4 shows the data in Fig. 3 modified to show relative pressure variations. Spectral analysis using Fast Fourier Transforms provides the results shown in Fig. 5. The two small peaks in amplitude are due to diurnal and semidiurnal tide effects. The reader is referred to Ref. 1 and Ref. 2 for more detail.

Multilayered Systems

A mathematical model was derived by S. Tariq[4,5] to satisfy the following conditions for a multilayered reservoir: each layer is horizontal and circular, homogeneous and isotropic, and bounded by impermeable formations at the top, bottom, and at the external drainage radius. Each layer has constant porosity and permeability, and

uniform thickness, but the drainage radius may be different for different layers. The fluid in each layer has small and constant compressibility. Initial reservoir pressure is the same for each layer; and instantaneous sandface pressure is identical for all layers. Pressure gradients are small and gravity effects negligible. The total production rate, q, is constant, but the production rate for each layer may vary in time. The model for n layers is specified by the following equations:

$$\frac{\partial^2 p_j}{\partial r^2} + \frac{1}{r}\frac{\partial p_j}{\partial r} = \frac{\phi_j \mu_j C_j}{k_j}\frac{\partial p_j}{\partial t}\ ;\ p_j(r,t) = p_i - p_j(r,t),\ r\varepsilon[r_{wj}, r_{ej}] \quad (5)$$

$$p_j(r,0) = 0 \quad (6)$$

$$\frac{\partial p_j}{\partial r}(r_{ej},t) = 0 \quad (7)$$

$$p_{wf}(t) = p_j(r_w,t) - S_j\left(r\frac{\partial p_i}{\partial r}\right)_{r_w} \quad (8)$$

$$q = C\frac{\partial p_{wf}}{at} + \sum_{j=1}^{n} q_j(t)$$

$$= C\frac{dp_{wf}}{dt} - 2\pi\sum_{j=1}^{n}\left(\frac{kh}{\mu}\right)_j\left(r\frac{\partial p_j}{\partial r}\right)_{r_{wj}} \quad (9)$$

where j = 1, 2, ..., n; s. = skin factor for each layer; and C = wellbore storage constant? cc/atm.

The system of equations is transformed into and solved in Laplace space. The resulting solution is then numerically inverted using the algorithm by Stehfest.[6]

A thorough analysis of drawdown data generated for different types of layered systems was conducted. The cases investigated included layers having different permeabilities, thicknesses, radii, and skin effects. Log-log type curves for analysis of multilayered systems were developed, and techniques for analyzing two-layered systems using semilog graphs of pressure vs time were described. The reader is referred to Ref. 4 and Ref. 5 for more detail.

Interference Testing

As more sensitive pressure gages have become available, interference testing, that is, observation of the pressure changes at a shut-in well resulting from a nearby producing well, has become feasible. Interference testing has the advantage of investigating more reservoir volume than a single-well test. For a producing well with considerable wellbore storage and skin effects, the combined effects of the storage and skin is to prolong the time it takes for the sandface flow rate to become equal to the surface flow rate. Since the sandface flow rate is not constant during this time period, conventional interference testing, which assumes a constant rate, is not valid.

The mathematical model used in this study by H. Sandal[7,8] assumes the flow is radial, the medium is infinite, homogeneous, and isotropic with constant porosity and permeability, the single-phase fluid is slightly compressible with constant viscosity, pressure gradients are small, and wellbore storage and skin are constant. The equations which represent this system are the following:

$$\frac{\partial^2 p_D}{\partial r_D^2} + \frac{1}{r_D}\frac{\partial p_D}{\partial r_D} = \frac{\partial p_D}{\partial t_D} \; ; \; p_D = p_D(r_D, t_D), \; r_D > 1, \; t_D > 0 \qquad (10)$$

$$p_D(r_D, 0) = 0 \; ; \; r_D > 1 \qquad (11)$$

$$C_D \frac{\partial p_{wD}}{\partial t_D} - \left.\frac{\partial p_D}{\partial r_D}\right|_{r_D=1} = 1 \; ; \; t_D > 0 \qquad (12)$$

$$p_{wD} = p_D - S \left.\frac{\partial p_D}{\partial r_D}\right|_{r_D=1} \; ; \; t_D > 0 \qquad (13)$$

$$\lim_{r_D \to \infty} p_D(r_D, t_D) = 0 \; ; \; t_D > 0 \qquad (14)$$

where p_D, r_D, t_D, and C_D are dimensionless pressure drop, radius, time, and storage, respectively, p_{wD} is the pressure drop inside the wellbore, and S is the wellbore skin factor.

The equations are transformed into and solved in Laplace space. The resulting Laplace space solution is numerically inverted using the Stehfest[6] algorithm.

Results were compared with the study by Garcia-Rivera and Raghavan[9] which was based on the superposition of a series of line source solutions combined with sandface flow rates obtained for a finite radius well (Ramey and Agarwal,[10] and Ramey, Agarwal, and Martin[11]). The comparison indicated that for low values of the effective wellbore radius, $C_D e^{2s}$, the Garcia-Rivera and Raghavan study may be in error. Figure 5 shows the close agreement between the two solutions for large values of $C_D e^{2s}$. Figure 6 shows an example of discrepancies between the two solutions. The reader is referred to Ref. 7 and Ref. 8 for more detail.

Steam/Water Relative Permeabilities

Using production data from the Wairakei field, R. Horne[12] and K. Shinohara[13] demonstrated that steam/water relative permeability curves can be generated from field data. The method of analysis was suggested by Grant,[14] but improvements were made on the production data. Specifically, assuming negligible wellbore heat loss, steam and water discharges at the wellbase were back calculated from the surface values. The wellbore heat loss was less than 1% in the well tested because they have been flowing for a long period of time. Total discharge values were divided by the wellhead pressure in order to filter out changes in discharge due only to pressure depletion in the reservoir. Thus, changes in discharge due to relative Permeability effects were isolated. The actual downhole temperature was used to determine fluid densities, viscosities, and enthalpies. Finally, flowing water saturation was determined from the back-calculated wellbase steam and water discharges. They did not take into account the immobile fluid in the reservoir.

Relative permeabilities were computed from equations for Darcy's law and the flowing enthalpy given below:

$$q_w = -\rho_w \frac{k}{\mu_w} F_w(S_w) A p' \tag{15}$$

$$q_s = -\rho_s \frac{k}{\mu_s} F_s(S_w) A p' \tag{16}$$

$$h = \frac{\rho_w h_w F_w(S_w)/\mu_w + \rho_s h_s F_s(S_w)/\mu_s}{\rho_w F_w(S_w)/\mu_w + \rho_s F_s(S_w)/\mu_s} \tag{17}$$

where q is the discharge rate, ρ is one-phase fluid density, μ is viscosity, A is flow area, p is the pressure gradient, F is the fractional flow, S_w is the flowing water saturation, and subscripts

s and w refer to the steam and water phases. Figure 7 shows the resulting permeability curves.

Future improvements on this method will include incorporation of wellbore heat loss in the back calculation of fractional flow, and use of irreducible water saturations estimated from results of experimental studies in the Stanford Geothermal Program.

Constant Pressure Production

Conventional well test analysis has been developed primarily for constant rate production. Since there are a number of common reservoir production conditions which result in constant pressure production, there is a need for a more thorough treatment of transient rate analysis and pressure buildup after constant pressure production.

In this work by C. Ehlig-Economides, the following assumptions are needed: flow is strictly radial, and the porous medium is homogeneous and isotropic, with constant thickness h, porosity ϕ, and permeability k. The fluid viscosity is constant, and the total compressibility of the fluid and the porous medium is small in magnitude and constant. The equations to be solved are the following:

$$\frac{\partial^2 p_D}{\partial r_D^2} + \frac{1}{r_D}\frac{\partial p_D}{\partial r_D} = \frac{\partial p_D}{\partial t_D} ; \quad p_D = p_D(r_D,t_D),\ r_D \varepsilon [1,R],\ t_D > 0 \qquad (18)$$

$$p_D(r_D,0) = 0 ; \ r_D \varepsilon [1,R] \qquad (19)$$

$$p_D(1,t) = 1 + S \lim_{r_D \to 1^+} \frac{\partial p_D}{\partial r_D} ; \ (t_D > 0) \qquad (20)$$

$$\lim_{r_D \to \infty} p_D(r_D,t_D) = 0 ; \ (t_D > 0) \text{ for unbounded reservoir} \qquad (21)$$

$$\frac{\partial p_D}{\partial r_D}(R,t_D) = 0 ; \ (t_D > 0) \text{ for closed bounded reservoirs, } R = \frac{r_e}{r_w} \qquad (22)$$

$$p_D(R,t_D) = 0 ; \ (t_D > 0) \text{ for constant pressure bounded reservoir} \qquad (23)$$

$$q_D(t_D) = - \lim_{rD \to 1^+} \frac{\partial p_D}{\partial r_D} \qquad (24)$$

where:

$$r_D = r/r_w,\quad t_D = \frac{kt}{\phi\mu c r_w^2},\quad p_D(r_D,t_D) = \frac{p_i - p(r_D,t_D)}{p_i - p_w},$$

$$q_D = \frac{q\mu}{2\pi kh(p_i - p_w)}, \text{ and } S \text{ is wellbore skin factor.}$$

Transient rate solutions have been tabulated in the literature. In this work, the numerical Laplace inverter by Stehfest[6] is used to generate solutions for the transient wellbore rate, the radial pressure distribution, and cumulative production including boundary and skin effects.

Pressure buildup after constant pressure production has not been properly handled in the literature. It can be shown that the following equation exactly represents pressure buildup after constant production under the conditions mentioned at the beginning of this section.

$$p_{DS}(\Delta t_D) = 1 + \int_{t_{Df}}^{t_{Df}+\Delta t_D} q_D(\tau)\,\frac{dp_{Dw}}{d\tau}\,(t_{Df}+\Delta t_D - \tau)\,d\tau \qquad (25)$$

where p_{DS} is the dimensionless shut-in pressure at the wellbore, t_{Df} is the flowing time before shut-in, Δt_D is the elapsed time after shut-in, q_D is dimensionless rate, defined above, and p_{Dw} is the dimensionless wellbore pressure drop for constant rate production, defined by:

$$p_{Dw}(t_D) = \frac{2\pi kh}{q\mu}\,(p_i - p[1,t_D]).$$

This work is nearing completion. The author may be consulted for more information,

Parallelepiped Model

The parallelepiped model has been proposed as a reasonable approximation for both The Geysers and the Italian geothermal reservoirs. Through use of source functions, Green's functions, and the Neumann product method described by Gringarten,[15] solutions are readily available for a number of related problems. The model assumes three-dimensional flow in a reservoir bounded by impermeable and/or constant pressure boundaries with a well located at any point which may be

fully or partially penetrated and which may intersect a horizontal or a vertical fracture. Solutions are in the form of infinite sums and integrals which must be integrated by computer. Type-curves are being developed which will shed new light on the behavior of geothermal reservoirs. In particular, detection of a boiling front may be possible in a dry steam reservoir bounded at its base by boiling water. This constitutes a constant pressure boundary if the reservoir is isothermal.

References

1. Arditty, P.C., and Ramey, H.J., Jr.: "Response of a Closed Well-Reservoir System to Stress Induced by Earth Tides," Paper SPE 7484, presented at the 53rd Annual Fall Meeting of the SPE of AIME, Oct. 1978, Houston, Texas.

2. Arditty, P.C.: "The Earth Tide Effects on Petroleum Reservoirs, Preliminary Study," Engineer's Degree Thesis, Stanford University Petroleum Engineering Department, 1978.

3. Bodvarsson, G.: "Confined Fluid as Strain Meters," J. Geoph. Res. (1970), 75, No. 14, p. 2711.

4. Tariq, S.M., and Ramey, H.J., Jr.: "Drawdown Behavior of a Well with Storage and Skin Effect Communicating with Layers of Different Radii and Other Characteristics," Paper SPE 7453, presented at the 53rd Annual Fall Meeting of the SPE of AIME, Oct. 1978, Houston, Texas.

5. Tariq, S.M.: "A Study of the Behavior of Layered Reservoirs with Wellbore Storage and Skin Effect," Ph.D. Dissertation, Stanford University Petroleum Engineering Department, 1977.

6. Stehfest, H.: "Numerical Inversion of Laplace Transforms," Communications of the ACM (Jan. 1970), 13, No. 1, Algorithm 368.

7. Sandal, H.J., Horne, R.N., Ramey, H.J., Jr., and Williamson, J.W.: "Interference Testing with Wellbore Storage and Skin Effect at the Produced Well," Paper SPE 7454, presented at the 53rd Annual Fall Meeting of the SPE of AIME, Oct. 1978, Houston, Texas.

8. Sandal, H.J.: "Interference Testing with Skin and Storage," Engineer's Degree Thesis, Stanford University Petroleum Engineering Department, 1978.

9. Garcia-Rivera, J., and Raghavan, R.: "Analysis of Short-Time Pressure Transient Data Dominated by Wellbore Storage and Skin at Unfractured Active and Observation Wells," Paper SPE 6546, presented at the 47th Annual California Regional Meeting of the SPE of AIME, Apr. 1977, Bakersfield, CA.

10. Ramey, H.J., Jr., and Agarwal, R.G.: "Annulus Unloading Rates and Wellbore Storage," Soc. Pet. Eng. J. (Oct. 1972), 453-462.

11. Ramey, H.J., Jr., Agarwal, R.G., and Martin, I.: "Analysis of 'Slug Test' or DST Flow Period Data," J. Can. Pet. Tech. (July-Sept. 1975), 34-47.

12. Horne, R.N., and Ramey, H.J., Jr.: "Steam/Water Relative Permeabilities from Production Data," Geothermal Resources Council, Trans. (July 1978), 2.

13. Shinohara, K.: "Calculation and Use of Steam/Water Relative Permeabilities in Geothermal Reservoirs, M.S. Report, Stanford University Petroleum Engineering Department, 1978.

14. Grant, M.A.: "Permeability Reduction Factors at Wairakei," presented at the AIChE-ASME Heat Transfer conference, Salt Lake City, Utah, Aug. 15-17, 1977.

15. Gringarten, A.C., and Ramey, H.J., Jr.: "The Use of Source and Green's Functions in the Solution of Unsteady Flow Problems in Reservoirs," Soc. Pet. Eng. J. (Oct. 1973), 285-296; Trans. AIME, 255.

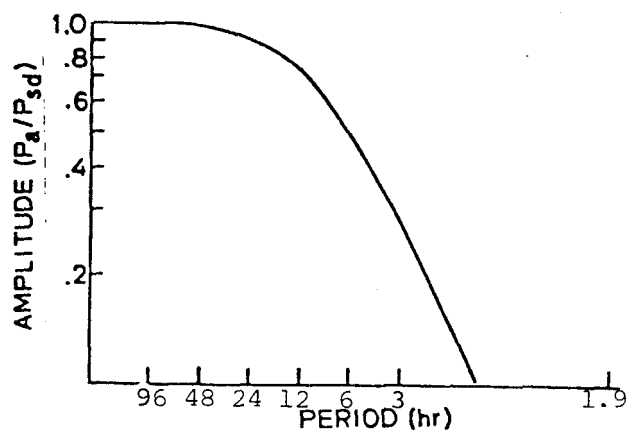

FIG. 1: RESPONSE (p_a/p_{SD}) OF A CLOSED-WELL RESERVOIR SYSTEM FOR A SANDSTONE CONTAINING GAS

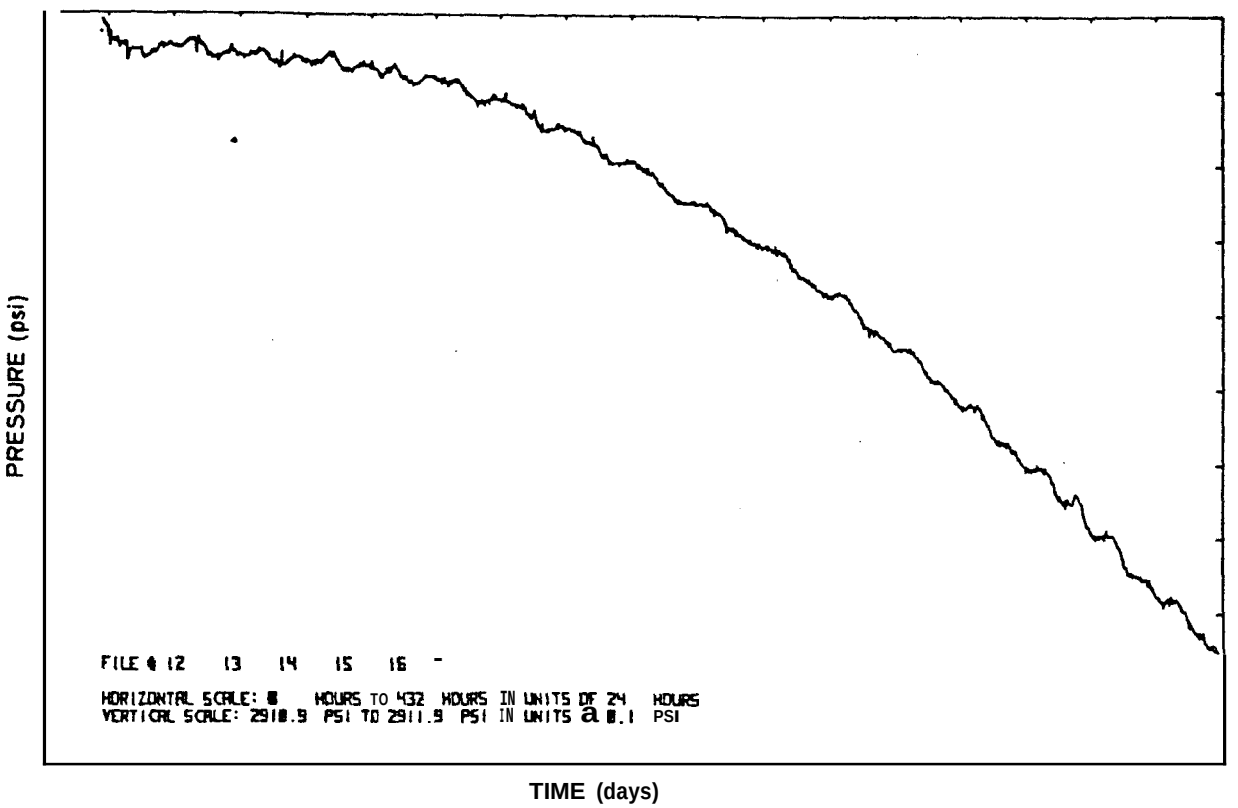

FIG. 2: INITIAL **DATA FOR** THE **"A" FIELD**

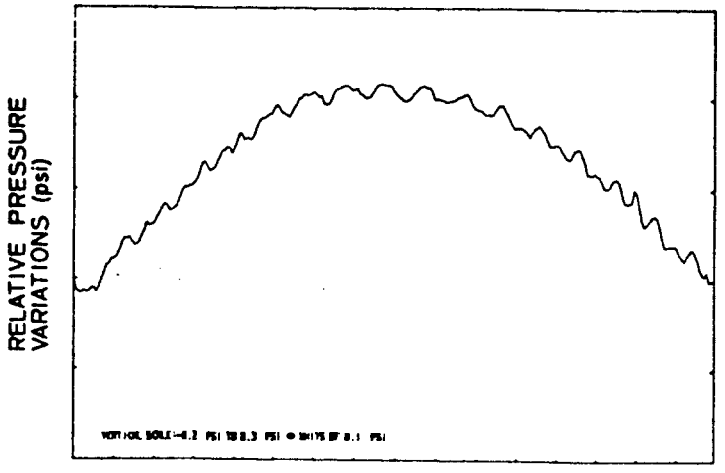

FIG. 3: MODIFIED DATA FOR THE "A" FIELD

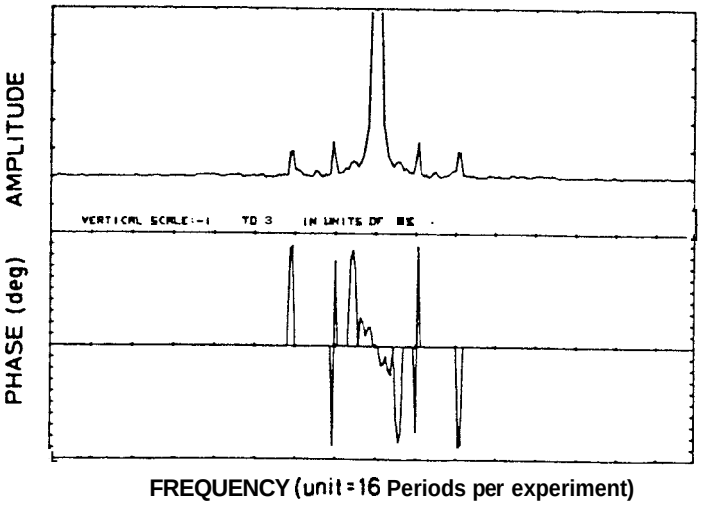

FIG. 4 : SPECTRUM ANALYSIS BY FFT FOR "A" FIELD

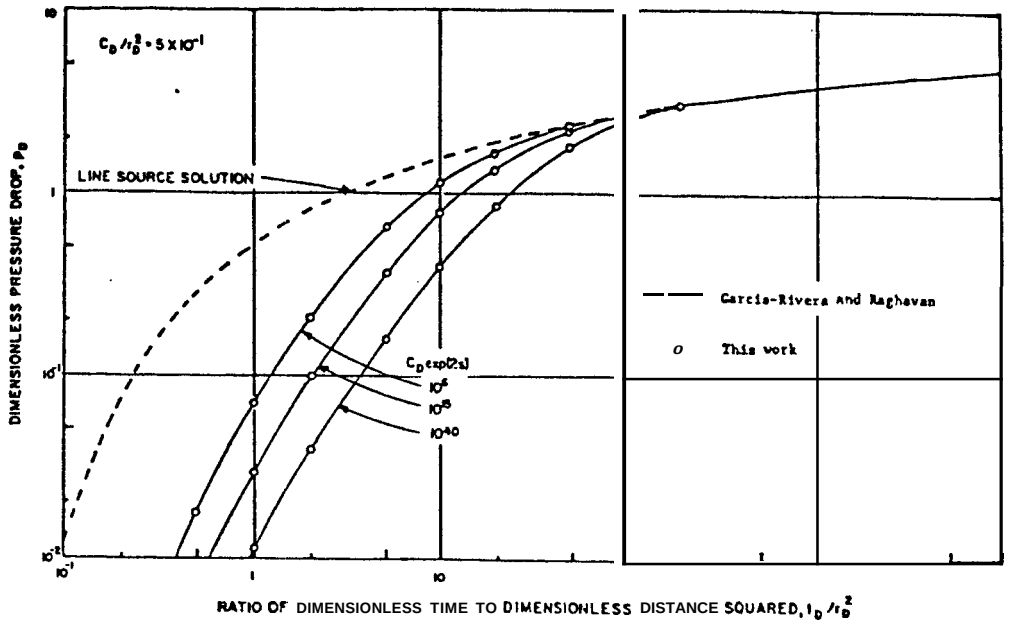

FIG. 5: COMPARISON OF RESULTS OF THIS STUDY WITH THE GARCIA-RIVERA AND RAGHAVAN STUDY

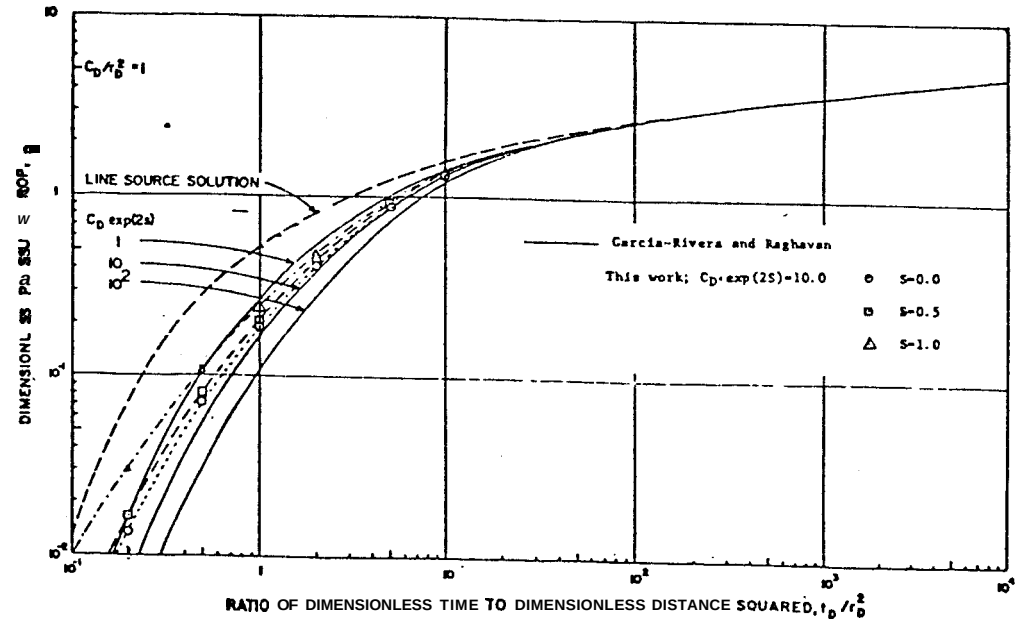

FIG. 6: COMPARISON OF RESULTS OF THIS STUDY WITH THE GARCIA-RIVERA AND RAGHAVAN STUDY

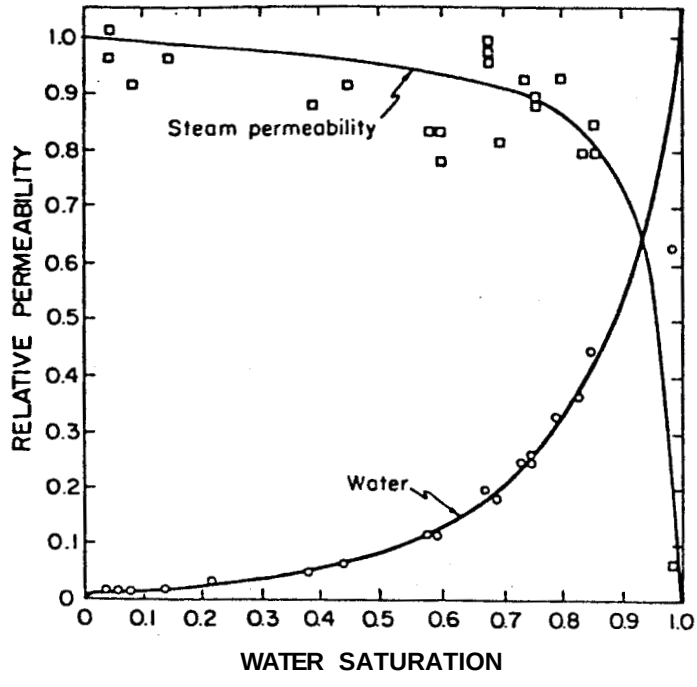

FIG. 7: STEAM-WATER RELATIVE PERMEABILITIES FROM WAIRAKEI WELL DATA

RECENT RADON TRANSIENT EXPERIMENTS

P. Kruger, L. Semprini, G. Cederberg, and L. Macias

Radon transient analysis is being developed as a method complementary to pressure transient analysis for evaluation of geothermal reservoirs. The method is based on the observations of Stoker and Kruger (1975) that radon concentration in produced geothermal fluids is related to geothermal reservoir type, production flow rates, and time. Stoker and Kruger showed that radon concentrations were markedly different in vapor-dominated and liquid-dominated systems, and varied not only among wells of different flow rate in an individual reservoir, but also varied timewise in individual wells. The potential uses of radon as an internal tracer for geothermal reservoir engineering were reviewed by Kruger, Stoker, and Umaña (1977). Also included were results of the first transient test performed with rapid flow rate change in a vapor-dominated field. The results of the next four radon-flow rate transient experiments were summarized by Kruger (1978) in which effects of well interference and startup production in a new well were demonstrated. Four of these first five radon transient experiments have been carried out in vapor-dominated reservoirs at The Geysers in California and Serrazzano in Italy. The systematics of the transients of radon concentration following abrupt changes in flow rate is being evaluated by Warren and Kruger (1978). The fifth test was at the HGP-A well in Hawaii, the first transient test in a liquid-dominated reservoir.

Three additional radon transient tests have been carried out, each in a different type of geothermal resource. The first test was in a petrothermal resource, the reservoir created by hydraulic fracturing by LASL in the hot, dry rock experiment in New Mexico. The results of this first 75-day production test of continuous forced circulation, during January-April, 1978, are given by Tester, et al (1978). The results of the radon concentration measurements made during this test are summarized by Kruger, Cederberg, and Semprini (1978). The second test was a second transient test at the HGP-A well in the liquid-dominated reservoir at Pohoiki, Hawaii, and the third test was a second transient test at the Grottitana well in the Serrazzano field at Larderello, Italy. The general observations of these tests are listed in Table 1. A summary of each of these three tests follows.

During the LASL hot dry rock flow test, five samples of recirculating production fluid were obtained by wellhead sampling. Two samples were obtained during the following shutin and venting periods of the test, and one sample of makeup water was analyzed during the test. The radon concentration data are given in Figure 1. The data show a quasi-exponential growth in radon concentration

TABLE 1

RECENT RADON TRANSIENT EXPERIMENTS

Site	Date	Test Conditions	Observations
LASL Hot, *Dry* Rock Fenton **Hill**, *New Mexico*	Spring, 1978	Recirculated water as forced circulation through hydraulic cracks	Logistics Growth of [Rn]
Univ. Hawaii **HGP-A** Pohoiki, Hawaii	(1) July, 1977 (2) July, 1978	**Short** period (∿ 4 hr) flow tests through two orifice sizes	(1) [Rn] constant with flow rate (2) [Rn]/Q growth with production?
ENEL Grottitana Serrazzano Italy	(1) Nov-Dec, 1976 (2) Aug-Sep, 1978	Long period (3 week) flow tests with two rapid changes in flow rate, Q	(1) [Rn]/Q constant (2) [Rn]/Q = $F(Q_{th})$?

during the 75-day test period. The first sample, collected 6 hours after initiation of the flow test period, was water resident in the large fracture volume during the prior 3-month shutin period and should represent geofluid radon in equilibrium with radon emanation from the fractured rock. The second sample indicated a dilution of this concentration with the large amount of makeup water required during the first 20 days of flow. The rise in concentration during the remainder of the test can be described by exponential growth of the form

$$[Rn] = [Rn]_o \; e+kt$$

where k is a growth constant with the value 0.035±0.005 for the first four samples. The fifth sample showed a value of k = 0.071 indicating a trend toward a logistics growth of the form shown in Figure 2 by

$$[Rn] = \frac{[Rn]^{\infty}}{1 + ae^{-bt}}$$

where $[Rn]^{\infty}$ is the infinite-time steady-state radon concentration for finite radium concentration and constant emanation and thermodynamic conditions; and a and b are empirical constants estimated by least-square fit as given in Figure 2. The value of $[Rn]^{\infty}$ = **11.2** nCi/l is based on the LASL measurement of [Ra]= 1.7 pCi/g in core rock and assumed values of emanating power, rock porosity and density, and the volumetric estimates of the fracture volume and total circulation volume. Four mechanisms for the observed quasi-exponential growth in radon concentration have been evaluated.

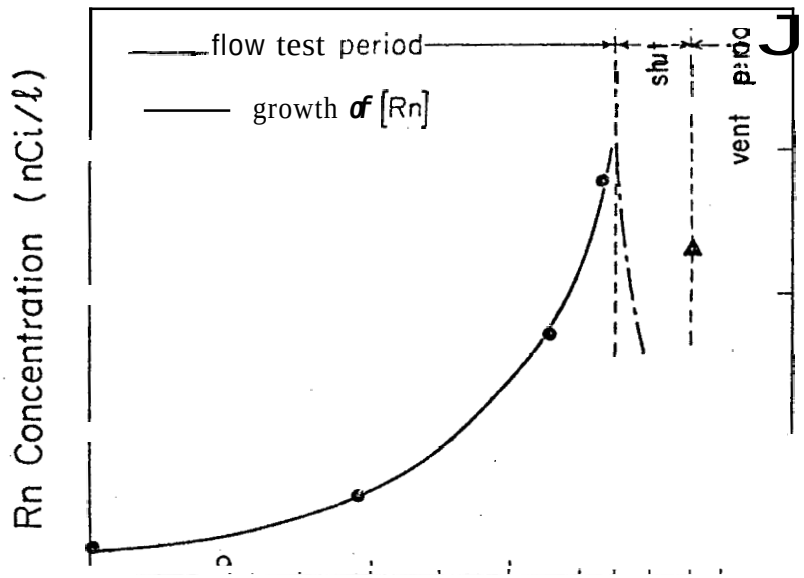

Fig test

Two of these, (1) the possibility of continuous radium dissolution and (2) the increase of radon solubility with decreasing reservoir temperature, have been discarded. The two remaining mechanisms, (3) an increase in emanating power of radon by recoil or diffusion from the rock to the recirculating fluid, or (4) an increase in the area of fractured rock surface (at constant emanating power) through increased fracturing of the formation by the recirculating fluid pressure and temperature differential cannot be distinguished. Current investigations by Macias (private communication) to determine the dependence on radon emanation on the pressure, temperature, and pore fluid density in fractured rock should assist in examining these two mechanisms.

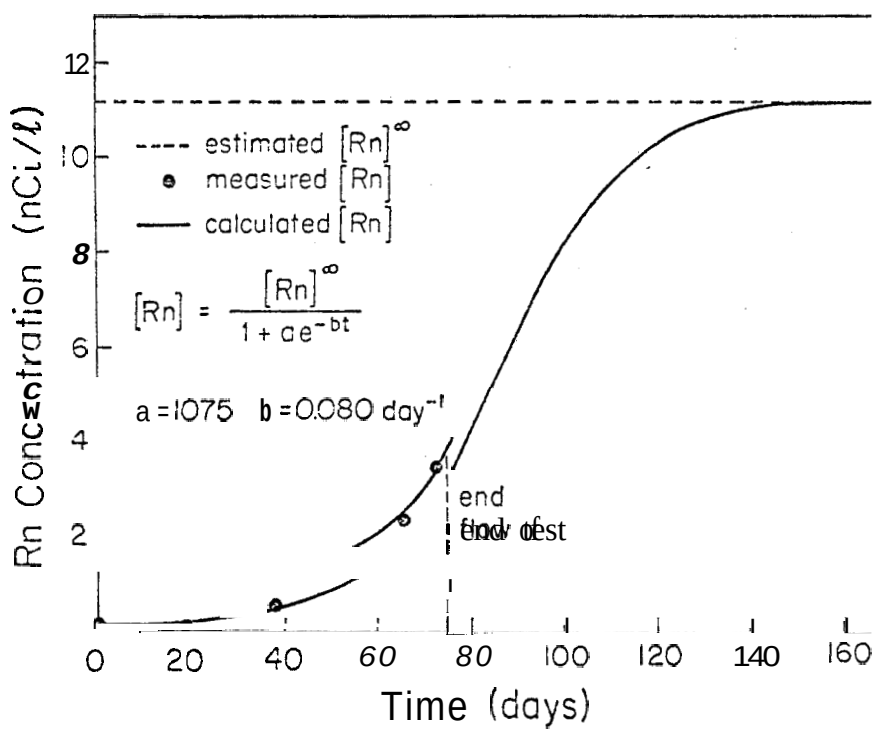

Figure 2. Logistics curve for Phase I radon data

The second test at the HGP-A well in Hawaii was run in July, 1978 in a manner similar to the first test of July, 1977 described by Kruger (1978). Both tests, with flow duration limited by environmental constraints, were run with changes in orifice plates to provide maximum flow through an 8" hole and minimum flow through a 1-3/4 - 2" hole. Flow rates were measured by the Russell James lip-flow pressure method (1962). The radon concentration and flow rate data are shown in Figure 3. Both short-period tests show essentially a constant radon concentration, independent of flow rate, in accordance with the horizontal flow model proposed by Stoker and Kruger (1975). However, the short flow periods preclude observation of any longer period transient. Several interesting trends are noted in the mean value data given in Table 2. primarily the increase in radon concentration per unit flow rate resulting from both an increase in mean radon concentration and a decrease in flow rate between the two tests. This observation may be consistent with the growth in radon concentration noted by Warren and Kruger (1978) for a newly producing well in a non-producing section of The Geysers geothermal field. If the model of "boil out" of condensed fluid near the wellbore is valid, observation of increased radon concentration per unit flow rate with further production in the HGP-A well can be predicted.

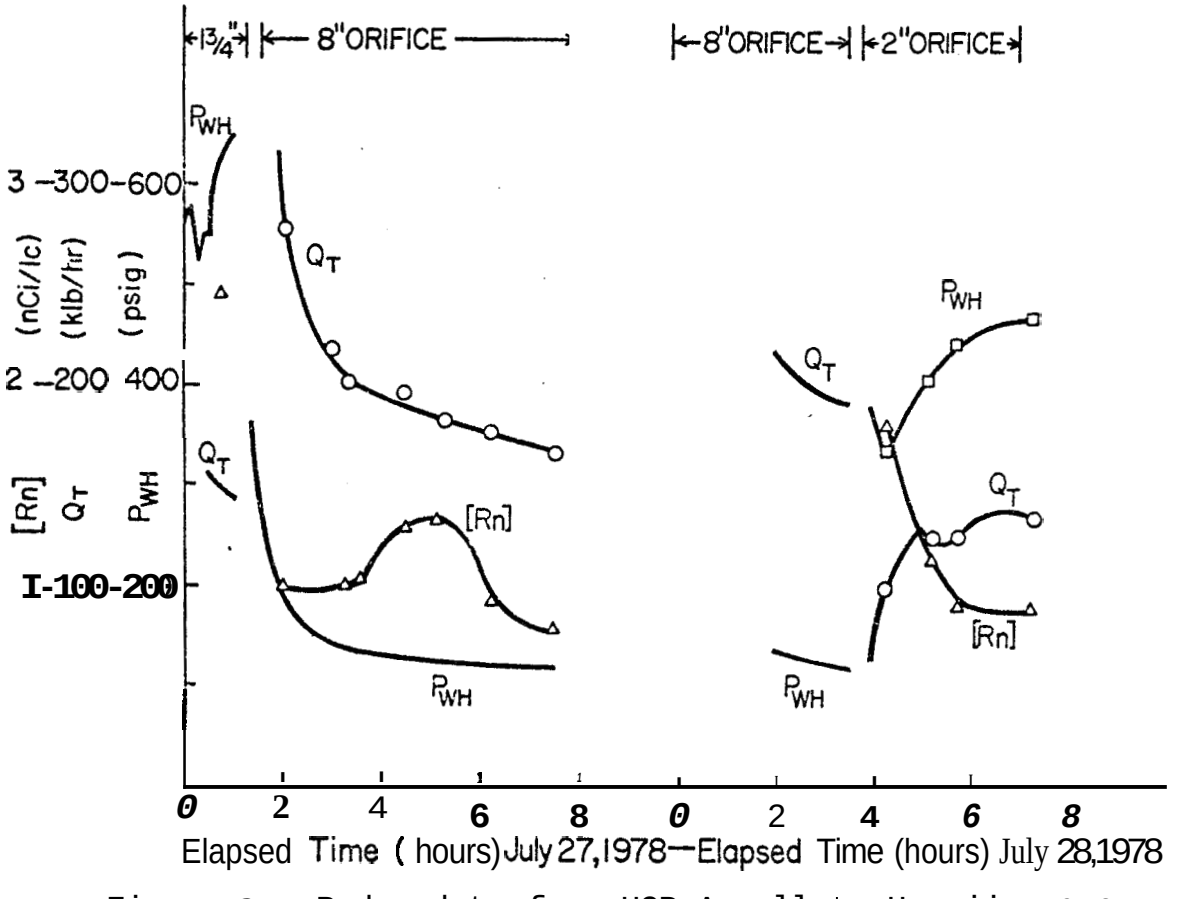

Figure 3. Radon data from HGP-A well in Hawaii, 1978

The second test at the Grottitana well at Serrazzano, Italy was run in August 1978 in cooperation with the **ENEL** staff in Castelnuovo. The preliminary results of this test, shown in Figure 4, agree well with the results of the November 1976 test, again showing a strong dependence of radon concentration on flow rate. However, Table 3 shows an interesting difference in this dependence related to the range of flow rates obtained. In the initial test, the flow rate was decreased from the full normal of about 11.8 t/hr to a value of about 7.5 t/hr. The observed transient was rapid (less than 1 day) and the radon concentration per unit flow rate was constant at a value of 7.33t0.76 over the entire flow rate range. In the current test, the flow rate was reduced in two stages, from **11.3** t/hr to **8.1** t/hr and then to about 5 t/hr. The two samples obtained for the first reduced flow rate showed a [Rn]/Q value in agreement with the previous value for the same flow rate change, but differed markedly for the lowest flow rate. Three possible physical reasons could account for this non-linear dependence on the lowest flow rate: (1) the increased reservoir pressures associated with the lowest flow rate sufficient to result in increased emanation from the reservoir rock (as indicated in the LASL hot dry rock experiment): (2) the possibility of a non-linear contribution from radon emanated from the boiling front to the well, as suggested for steam systems by Warren and Kruger (1978); and (3) the possibility of partial condensation of the steam under subcooled conditions during transit to the well. Here again the experimental data of Macias on emanation under known reservoir conditions will be of value in distinguishing between these possibilities.

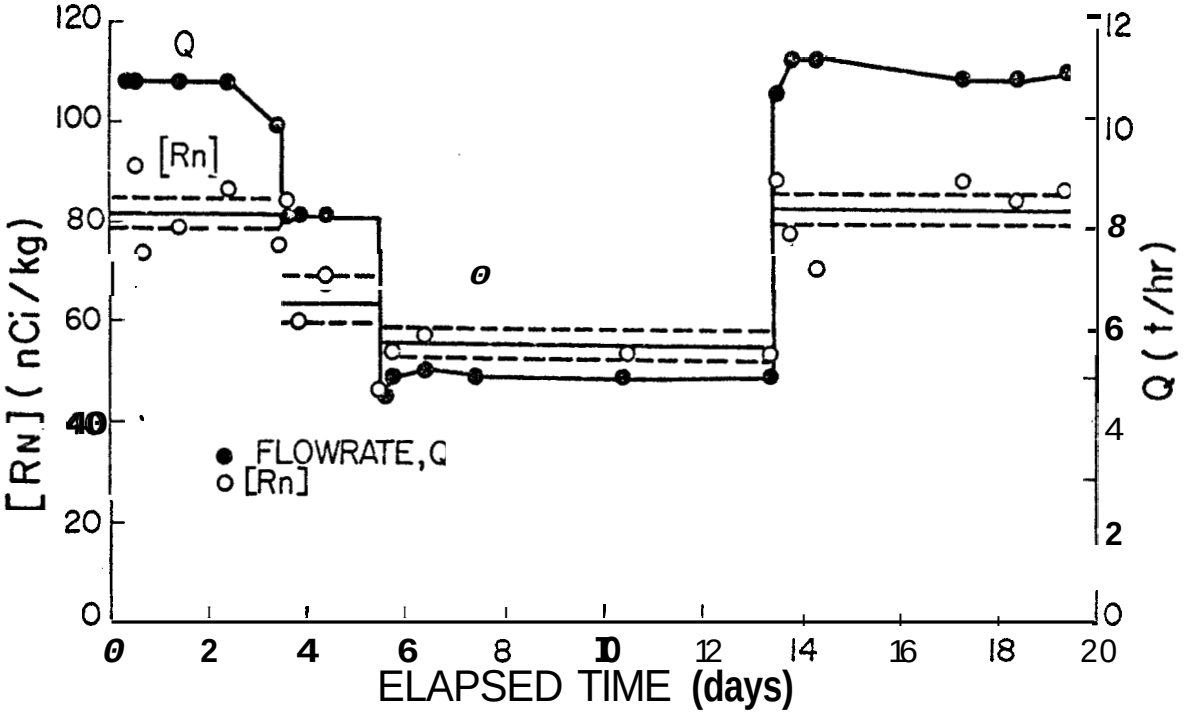

Figure 4. Radon data from Grottitana Well, Italy

TABLE 2

RADON TRANSIENT TESTS - POHOIKI, HAWAII

Date	Orifice (inches)	$\bar{Q}$ (klb/hr)	$[\bar{Rn}]$ (nCi/kg)	$[\bar{Rn}]/Q$ ($\frac{pCi/kg}{mt/hr}$)
July, **1977**	**8**	*286*	**0.89**	**1.41**
	1-3/4	**137**	**0.85**	2.82
July, **1978**	**8**	201	1.22	**2.76**
	2	121	1.20	**4.50**

TABLE 3

RADON TRANSIENT TESTS - GROTTITANA, ITALY

Test Dates	[Rn]/Q Ratio	Q Range (t/hr)
Nov - Dec **1976**	**7.33 ± 0.76**	**7.5 - 11.8**
Aug - Sep **1978**	**7.8 ± 0.3**	**8.1 - 11.3**
	11.5 ± 0.6	**4.6 - 5.0**

REFERENCES

James, R. (1962), Steam-Water Critical Flow through Pipes, Inst. Mech. Engrs. Proc. **176**, No. 26, **741.**

Kruger, P. (1978), Radon in Geothermal Reservoir Engineering, Trans. Geothermal Resources Council 2, **383-385.**

Kruger, P., G. Cederberg, and L. Semprini (1978), Radon Data - Phase **I** Test LASL Hot Dry Rock Project, Tech. Report SGP-TR-27.

Kruger, P., **A.** Stoker, and A. Umaña (1977), Radon in Geothermal Reservoir Engineering, Geothermics 5, 13-19.

Stoker, A. and P. Kruger (1975), Radon in Geothermal Reservoirs, Proceedings Second U. N. Symposium on the Development and Use of Geothermal Resources, San Francisco, CA.

Tester, J., et al (1978), Report on Phase **I** Test Results, LASL Hot Dry Rock Project, in preparation.

Warren, G. and P. Kruger (1978), Radon in Vapor Dominated Geothermal Reservoirs, Tech. Report SGP-TR-22, in preparation.

ENERGY RECOVERY FROM FRACTURE-STIMULATED GEOTHERMAL RESERVOIRS

A. H. Hunsbedt, * R. Iregui, P. Kruger, and A. L. London

Stanford Geothermal Program

Stanford University

Stanford, CA 94305

Submitted to
18th ASME-AIChE National Heat Transfer Conference
Special Session on
Heat Transfer in Geothermal Systems
San Diego, CA
August 5-8, 1979

ENERGY RECOVERY FROM FRACTURE-STIMULATED GEOTHERMAL RESERVOIRS: PART I - ANALYTIC MODELS

by

A. H. Hunsbedt,* R. Iregui, P. Kruger, and A. L. London
Stanford Geothermal Program
Stanford University
Stanford, CA 94305

ABSTRACT

Large quantities of thermal energy are stored in he earth's crust, much of it in the form of petrothermal deposits (hot dry rock). The extraction of this energy is presumably uneconomical because of low permeabilities. Future developments may show that it is practical to fracture such hot rock artificially by high energy explosives and hydraulic thermal stress cracking techniques. To show the potential for stimulated petrothermal resources, energy extraction processes and extraction efficiencies were studied in a laboratory model of artificially fractured rock systems. Preliminary rock heat transfer models were developed which showed the need for a more comprehensive analytic technique to describe the heat transfer from a collection of irregularly shaped rocks of various sizes under artibrary cooling conditions. The development of such a rock heat transfer model is presented in this paper. The model is valid for all Biot numbers. Comparison of rock thermal transients measured in the laboratory model experiments are in satisfactory agreement with model predictions. The problems of water heating while flowing through the hot rock media was also examined. An analytic model of this process, referred to as the sweep process, is also presented. Comparison of model predictions to laboratory experiment results also showed satisfactory agreement. Application of the sweep model to examine the energy extraction potential from fracture-stimulated geothermal reservoirs as a function of rock size and water flow rate are presented in Part II of this paper.

ENERGY RECOVERY FROM FRACTURE-STIMULATED GEOTHERMAL RESERVOIRS: PART II - APPLICATIONS

by

A. H. Hunsbedt,* R. Iregui, P. Kruger, and A. L. London
Stanford Geothermal Program
Stanford University
Stanford, CA 94305

ABSTRACT

A model of the heating that occurs when originally cold water is flowing through a fractured geothermal reservoir under high pressure from an injection point to a distant production point was presented in Part I of this paper. This water sweep process is being considered for use in extracting the large quantities of thermal energy in the hot rock geothermal energy deposits following artificial fracturing by high energy explosives or hydraulic/thermal stress cracking techniques. The sweep model was developed in terms of a non-dimensional parameter called the number of transfer units which is the ratio of water residence time and time constant of the effective rock size. A parametric study was carried out to investigate the effect.